ISSN 1936-878X/$36.00
PUBLISHED BY ELSEVIER INC.
DOI:10.1016/j.jcmg.2010.05.014

Fused Whole-Heart Coronary and Myocardial Scar Imaging Using 3-T CMR

Implications for Planning of Cardiac Resynchronization Therapy and Coronary Revascularization

James A. White, MD,*†‡ Nowell Fine, MD,* Lorne J. Gula, MD, MSc,* Raymond Yee, MD,* Mohammed Al-Admawi, MD,* Qi Zhang, PhD,† Andrew Krahn, MD,* Allan Skanes, MD,* Anna MacDonald,* Terry Peters, PhD,†§ Maria Drangova, PhD†§

London, Ontario, Canada

OBJECTIVES The aim of this study was to demonstrate the feasibility of providing spatially matched, 3-dimensional (3D) myocardial scar and coronary imaging for the purpose of fused volumetric image display in patients undergoing cardiac resynchronization therapy (CRT) or coronary artery revascularization (CAR).

BACKGROUND Clinical success in coronary vascular-based interventions is mitigated by the presence of scar in related myocardium. Pre-procedural fused volumetric imaging of both myocardial scar and coronary vasculature may benefit pre-procedural planning and patient selection in populations referred for CRT or CAR.

METHODS A total of 55 studies were performed in patients referred for either CRT (n = 42) or CAR (n = 13). Coronary-enhanced and scar-enhanced imaging was performed on a 3-T cardiac magnetic resonance scanner using the same cardiac-gated, 3D, free-breathing cardiac magnetic resonance technique during and 20 minutes following slow gadolinium infusion. Matched image datasets were fused and volume-rendered to simultaneously display coronary anatomy and myocardial scar. Visual scoring of coronary artery, coronary vein, and myocardial scar image quality (score 0 to 4) was performed. The clinical impact of imaging was also scored using a physician survey.

RESULTS Mean age was 57 ± 14 years. Combined 3D coronary and scar imaging was successful in 49 studies (89%). A quality score ≥2 was obtained for 97% of proximal- and mid-coronary artery and vein segments. The mean quality score of 3D scar imaging was 2.8 ± 1.0 and was scored as ≥2 in 86% of patients with myocardial scar. All patients with a scar quality score ≥2 achieved successful image fusion. Transmural scar was present below ≥1 planned target vessel in 9 patients (39%) planned for CRT and 8 patients (62%) planned for CAR. Physician surveys demonstrated incremental clinical impact in 67% of patients.

CONCLUSIONS Three-dimensional myocardial scar and coronary imaging with fused volumetric display is clinically feasible and may be valuable for the planning of vascular-based interventions when regional myocardial scar is pertinent to therapeutic success. (J Am Coll Cardiol Img 2010;3:921–30)

From the *Division of Cardiology, Department of Medicine, Schulich School of Medicine and Dentistry, University of Western Ontario, London, Ontario, Canada; †Imaging Research Laboratories, Robarts Research Institute, University of Western Ontario, London, Ontario, Canada; ‡Lawson Health Research Institute, University of Western Ontario, London, Ontario, Canada; and the §Departments of Medical Biophysics and Medical Imaging, University of Western Ontario, London, Ontario, Canada. Dr. White is a clinician scientist and Dr. Drangova is a career scientist with the Heart and Stroke Foundation of Ontario. Funding for the research was provided in part by the Heart and Stroke Foundation of Ontario grant NA 6488 (to Dr. White) and the Canadian Foundation for Innovation Leaders opportunity fund 18847 (to Dr. White). Dr. White receives in-kind research contributions from Bayer Inc. in the form of CMR contrast agents. All other authors report that they have no relationships to disclose.

Manuscript received September 28, 2009; revised manuscript received April 26, 2010, accepted May 3, 2010.

Patients with reduced left ventricular (LV) systolic function are frequently considered for vascular-based interventions aimed at improving regional and global systolic performance. Both cardiac resynchronization therapy (CRT) and coronary artery revascularization (CAR) rely upon appropriate vascular targets in the venous and arterial circulations, respectively. Three-dimensional (3D) vascular imaging has been shown to be of value for identification of these targets (1–5). However, the clinical benefit of both procedures also appears reliant upon regional myocardial scar. Transmural scar in myocardial segments targeted

See page 931

for either CRT lead placement or CAR mitigates the benefit of these therapies (6–10). Therefore, although anatomic imaging may assist in identifying appropriate vascular targets, the health of associated myocardial targets must also be considered. A combined 3D imaging technique, spatially registering both myocardial scar and vascular anatomy, may offer advantages for the planning of such procedures.

In this study, we demonstrate both the clinical feasibility and clinical impact of performing fused, 3D myocardial scar and coronary vascular imaging in patients being evaluated for CRT or CAR.

ABBREVIATIONS AND ACRONYMS

3D = 3-dimensional
CAR = coronary artery revascularization
CMR = cardiac magnetic resonance
CRT = cardiac resynchronization therapy
DE = delayed enhancement
LV = left ventricle/ventricular
MRA = magnetic resonance angiography

METHODS

Subjects and image acquisition. Fifty-five consecutive studies were performed in 53 patients being evaluated for CRT or CAR. Two patients had repeat imaging performed following CAR. Patients with standard contraindications to cardiac magnetic resonance (CMR) or with a glomerular filtration rate ≤45 ml/min/1.73 m^2 were excluded. All patients provided written informed consent. The study was approved by the local institution's Research Ethics Board.

A 3-T CMR scanner (TRIO, Siemens Medical Systems, Erlangen, Germany) and 6-element body surface receiver coil were used. Cine imaging was first performed using a steady-state free precession–based pulse sequence in serial short-axis slices from the atrioventricular annulus to the apex at 10-mm intervals and in long-axis orientations (slice thickness 6 mm, gap 4 mm, echo time 1.5 ms, repetition time 3.0 ms, flip angle 50°). A 3D whole-heart, inversion-recovery gradient echo pulse sequence with a respiratory navigator pulse placed over the right hemidiaphragm was used to obtain both an early (coronary-enhanced) and late (scar-enhanced) dataset (voxel size 1.3 × 1.3 × 1.3 mm^3, echo time 1.3 ms, flip angle 20°, integrated parallel acquisition technique 2). Fat saturation was employed to suppress pericardial fat signal. Imaging volumes were prescribed in the transverse plane from the aortic arch to below the most inferior aspect of the heart (slab thickness 120 to 144 slices) based on multiplanar scout images. Adjustment of trigger delay and number of segments was performed to maintain image acquisition between the onset and termination of cardiac standstill, as determined from the 4-chamber cine.

For coronary-enhanced imaging, an intravenous infusion of 0.2 mmol/kg gadolinium (Magnevist, Bayer Inc., Toronto, Ontario, Canada) was given at 0.3 ml/s, followed by 40 ml of saline at the same rate. Imaging was initiated 25 s following infusion onset, as previously described (11). A repeat (scar-enhanced) dataset was then acquired 20 to 25 min later (Online Video 1), with adjustment of the inversion time (TI) to provide optimal myocardial signal suppression. The TI was set at 200 ms for coronary-enhanced imaging and was adjusted for scar-enhanced imaging (typical range 240 to 270 ms), as previously described (12). These adjustments were performed using a test-image slab (10-mm thickness) acquired over the mid-ventricle. The acceptance rate of the respiratory navigator was recorded for both full-volume acquisitions.

To provide for visual and quantitative comparisons of 3D delayed enhancement (DE) imaging with conventional DE techniques, a series of standard short-axis 2-dimensional (2D) DE images was also obtained between coronary-enhanced and scar-enhanced 3D imaging. This was performed using a standard phase-sensitive inversion recovery pulse sequence (matrix 256 × 192, slice thickness 6 mm, gap 4 mm).

CMR image interpretation. Serial short-axis cine images were evaluated using semiautomated software (CMR42, Circle International, Calgary, Alberta, Canada) to obtain LV end diastolic volume, LV end systolic volume, and ejection fraction. To provide a representation of average scar burden, quantitative analysis of 2D short-axis DE images was also performed with scar defined as signal ≥5 SD above the mean signal of normal remote myocardium.

Coronary-enhanced and scar-enhanced 3D datasets were evaluated using open source software

(OsiriX, version 3.5.1, 2009, OsiriX Imaging Software, Geneva, Switzerland) (13). An experienced, blinded observer visually scored each dataset using a 3D multiplanar reformatted display. Coronary vessel image quality was scored using a 14-segment coronary artery model (14,15) and a 7-segment coronary vein model, as shown in Figure 1. A 5-point scoring system was used as follows: 0 = noninterpretable, 1 = poor quality, 2 = medium quality, 3 = good quality, and 4 = excellent quality. All segments assigned a value of 0 (noninterpretable) or 1 (poor) were considered clinically "nonevaluable."

The 3D scar-enhanced datasets were visually scored for image quality using the same 5-point system. A score of ≥2 (interpretable) was assigned only if the extent and distribution of signal enhancement on 3D scar imaging was assessed to accurately reflect standard 2D DE imaging. Additionally, to provide quantitative validation of the 3D DE technique to conventional 2D imaging, we randomly selected 20 patients with myocardial scar and reformatted their 3D DE datasets into a series of short-axis, mean signal intensity slabs (thickness 6 mm, gap 4 mm). This was followed by an identical quantitative signal analysis, as was performed for 2D DE images with total scar volumes, and then correlated between the 2 techniques.

Image fusion technique. Matched 3D coronary and scar-enhanced datasets were evaluated using a synchronized display (OsiriX, version 3.5.1, OsiriX Imaging Software) (13). A seeded, 3D region growing technique was used to segment myocardial scar from 3D scar-enhanced datasets with a signal ≥5 SD above normal, remote myocardium included as scar. If segmentation was found to leak into the adjacent blood pool, a higher threshold of 8 SD was then adopted (required in 4 studies). Segmented scar volumes were fused to spatially matched coronary datasets and volume rendered for visualization purposes (Fig. 2, Online Videos 2A and 2B).

Evaluation of clinical relevance. For all successfully fused datasets, the presence of transmural scar (≥50% wall thickness) in ≥1 myocardial segment below a target vessel(s) was determined. The largest-diameter coronary vein of the posterolateral wall was assumed to be the target vessel for patients undergoing CRT. For patients undergoing CAR, all arterial segments containing or distal to an obstructive coronary lesion(s) were assumed to be the target vessel(s). The presence of obstructive arterial lesions (≥70% stenosis) was determined from invasive coronary angiography and was assigned to segments using a 14-segment artery model.

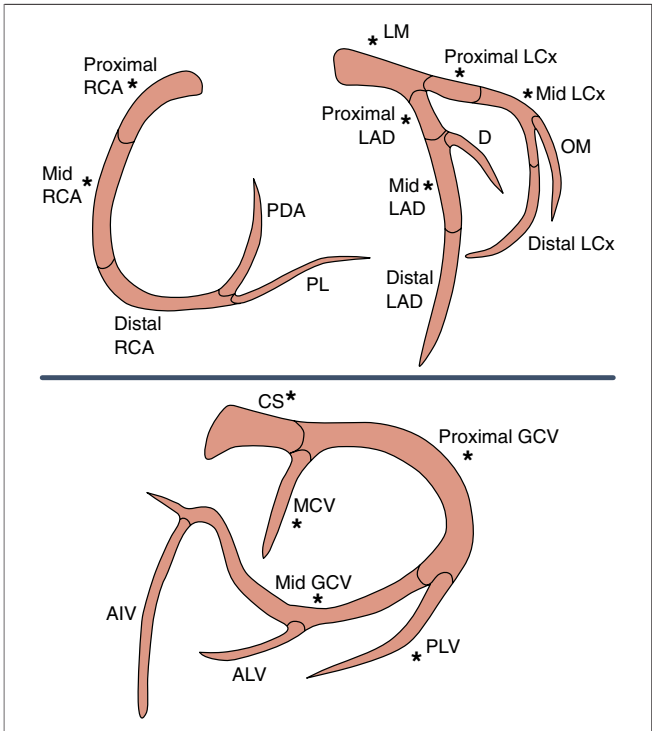

Figure 1. Illustration of Coronary Artery and Vein Segmentation Models Used for Image Analysis

Fourteen-segment coronary artery **(upper)** and 7-segment coronary vein **(lower)** scoring models. *Segments classified as proximal-mid (all others classified as distal-branch vessels). AIV = anterior interventricular vein; ALV = anterolateral vein; CS = coronary sinus; GCV = great cardiac vein; LAD = left anterior descending; LCx = left circumflex; LM = left main; MCV = middle cardiac vein; OM = obtuse marginal; PDA = posterior descending artery; PLA = posterior lateral artery; PLV = posterolateral vein; RCA = right coronary artery.

To evaluate the incremental impact of fused scar–coronary imaging on therapeutic decision making, the referring physician was provided a descriptive report identifying which target vessel(s) had underlying scar and the transmural extent of this scar. Representative 3D fused images were also provided. The physician was asked to score the impact of this report on the planned procedure using a 5-point scale as follows: 0 = negative impact (led to confusion), 1 = no impact, 2 = modest impact (change in anticipated benefit but no change in planned therapy), 3 = moderate impact (change in the vessel[s] to be targeted), 4 = major impact (cancellation of procedure). A score of ≥2 was considered to be a clinically significant impact.

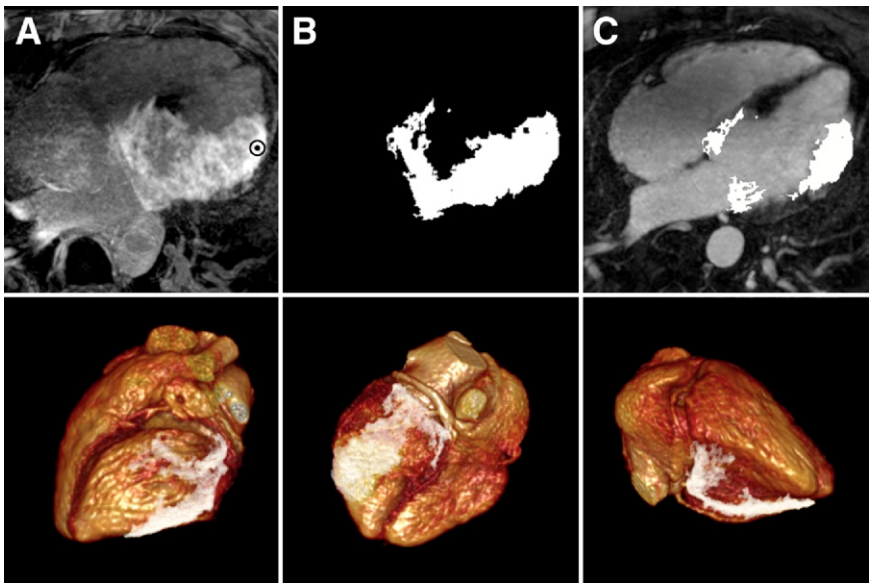

Figure 2. 3D Scar Segmentation and Image Fusion Technique

(A) Three-dimensional (3D) scar data reviewed (shown as thick maximum intensity projection) and "seed" (⊙) placed in central region of scar. **(B)** 3D region growing algorithm applied and segmented data generated. **(C)** Segmented data fused to matched coronary magnetic resonance angiography data. **Bottom row** shows volume-rendered images of a fused dataset demonstrating a large inferior wall myocardial infarction from a mid–right coronary artery vessel occlusion.

Statistical analysis. Data were expressed as mean values ± SD. Statistical analyses were performed using a commercially available software program (GraphPad Prism, version 5.0, GraphPad Software, San Diego, California). The proximal to mid coronary artery and coronary vein segments, indicated in Figure 1, were considered to be most clinically relevant for procedural planning and were reported separately for quality scoring. Comparisons of categoric variables (quality score) were performed by means of a 2-tailed *t* test, as indicated in the Results section. A probability value ≤0.05 was considered significant.

RESULTS

Baseline patient and CMR characteristics are listed in Table 1. Forty-two studies were performed in patients being evaluated for CRT and 13 for CAR. The mean age was 57 ± 14 years, and 11 patients (21%) were female. Obstructive coronary artery disease (stenosis ≥70%) was documented on prior invasive angiography in 30 patients (57%), with all other patients having a diagnosis of nonischemic cardiomyopathy. The mean ejection fraction was 43 ± 17%. The mean heart rate at time of CMR was 73 ± 13 beats/min (range 45 to 102). All patients were in sinus rhythm with the exception of 1 (rate-controlled atrial fibrillation), and 8 patients had frequent ventricular ectopy during image acquisition.

The combined 3D scar and coronary imaging protocol was completed in 49 of 55 studies (36 of 42 CRT studies [86%] and 13 of 13 CAR studies [100%]). Imaging was not completed in 3 studies because of inconsistent breathing pattern, in 2 because of frequent ectopy, and in 1 because of an inability to lie flat. The mean imaging time for the coronary and scar-enhanced data sets was 6 min, 45 s, and 6 min, 18 s, respectively.

Forty-four studies (80%) from 42 patients demonstrated the presence of myocardial scar. The pattern of scarring was ischemic (subendocardial based) in 28 studies (64%), midwall in 9 studies (20%), and epicardial based in 7 studies (16%). Seven studies (16%) had a combined ischemic/nonischemic scar pattern. The mean burden of myocardial scar in the population was 13 ± 12% of the LV mass.

Coronary artery imaging. Of 686 possible coronary artery segments, 682 were visually scored (Table 2). In 4 segments, no lumen was identifiable, suggesting complete occlusion without retrograde filling (confirmed in all cases by invasive coronary angiography).

Table 1. Patient and CMR Characteristics

Patient characteristics	
Age (yrs)	57 ± 14
Female	11 (21%)
BMI (kg/m^2)	28 ± 5
Hypertension	25 (47%)
Diabetes mellitus	7 (13%)
Hyperlipidemia	24 (45%)
Current smoker	17 (32%)
Etiology of LV dysfunction	
Obstructive CAD*	30 (57%)
Nonischemic (no obstructive CAD*)	23 (43%)
CMR characteristics	
Cardiac rhythm during CMR	
Sinus rhythm	54 (98%)
Frequent PVCs	8 (15%)
Atrial fibrillation	1 (2%)
Mean heart rate (beats/min)	73 ± 13
LVEF (%)	43 ± 17
LV EDV (ml)	198 ± 107
LV ESV (ml)	130 ± 99
LV mass (g)	142 ± 65
Myocardial scar	
Any	44 (80%)
Subendocardial based	28 (51%)
Midwall	9 (16%)
Epicardial based	7 (13%)
Total scar volume† (% of LV mass)	13 ± 12

Values are mean ± SD or n (%). *Defined as ≥70% stenosis in major epicardial coronary artery by invasive catheterization. †Defined as ≥5 SD above the mean signal of normal myocardium.

BMI = body mass index; CAD = coronary artery disease; CMR = cardiac magnetic resonance; EDV = end diastolic volume; ESV = end systolic volume; LV = left ventricle; LVEF = left ventricular ejection fraction; PVC = premature ventricular complex.

Example coronary artery images are shown in Figure 3A. Quality scores ≥2 (clinically evaluable) were achieved in 333 of 343 (97%) proximal-mid arterial segments (Table 2). Quality scores for the proximal-mid segments and distal-branch segments are shown in Table 3.

Table 2. Number of Evaluable Segments (Quality Score ≥2 of the Coronary Arteries and Coronary Veins)

Coronary Segment	Evaluable Segments (%)
Coronary arteries	
Proximal and mid-segments	333/343 (97)
Distal and branching segments	303/339 (89)
Total coronary arteries	636/682 (93)
Not assessed*	4
Coronary veins	
Proximal and mid-segments	237/245 (97)
Distal segments	87/98 (89)
Total coronary veins	324/343 (95)

*No lumen visualized, chronic occlusion without distal collateral flow and confirmed by invasive coronary angiogram.

Coronary vein imaging. Examples of coronary vein images are shown in Figure 3B. A total of 343 coronary vein segments were visually assessed. A quality score of ≥2 (clinically evaluable) was achieved in 237 of 245 (97%) proximal-mid segments (Table 2). Mean quality scores are shown in Table 3.

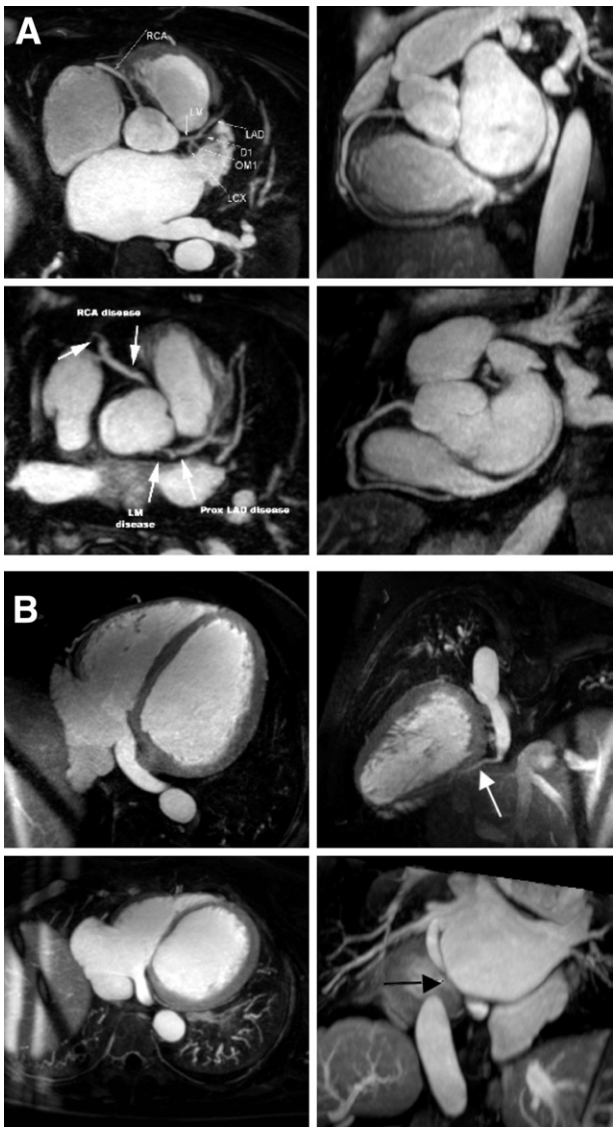

Figure 3. Examples of 3D Contrast-Enhanced Coronary MRA Studies

(A) Normal **(top row)** and abnormal **(bottom row)** coronary artery systems. **(B)** Normal **(top row)** and abnormal **(bottom row)** coronary vein systems (**white arrow** indicates a posterolateral vein and **black arrow** indicates severe reduction in lumen diameter of the great cardiac vein). MRA = magnetic resonance angiography; other abbreviation as in Figure 2.

Table 3. Visual Quality Scoring of Coronary Artery, Coronary Vein, and High-Resolution 3-Dimensional Scar Images

Cardiac Structure	Mean Quality Score
Coronary artery segments	
All proximal and mid-segments	3.1 ± 0.8
Left main artery	3.3 ± 0.6
Proximal left anterior descending artery	3.2 ± 0.7
Mid-left anterior descending artery	3.1 ± 0.7
Proximal right coronary artery	3.2 ± 0.7
Mid-right coronary artery	3.1 ± 0.9
All distal and branch segments	2.3 ± 0.8
Distal left anterior descending artery	2.7 ± 0.9
First diagonal branch	2.4 ± 0.7
Distal left circumflex	2.2 ± 0.8
First obtuse marginal branch	2.1 ± 0.8
Distal right coronary artery	2.8 ± 0.9
Posterior descending artery	2.0 ± 0.7
Posterolateral artery	1.8 ± 0.8
Coronary vein segments	
All proximal and mid-segments	3.3 ± 0.9
Coronary sinus	3.7 ± 0.6
Proximal great cardiac vein	3.5 ± 0.8
Posterolateral vein	2.9 ± 0.9
Mid-great cardiac vein	3.0 ± 0.9
Middle cardiac vein	3.2 ± 0.9
All distal and branch segments	2.6 ± 0.8
Anterolateral vein	2.1 ± 0.8
Anterior interventricular vein	3.1 ± 0.8
Myocardial scar	2.8 ± 1.0

Values are expressed as mean ± SD.

3D scar imaging. Examples of 3D scar-enhanced imaging are shown in Figure 4. Myocardial scar was seen on 44 of 49 3D datasets and visually corresponded to the distribution of scar seen on standard 2D imaging in all cases. The mean quality score of these studies was 2.8 ± 1.0 (Table 3). A quality score ≥2 was reported in 38 studies (86%), obtained from 36 patients. All images with quality scores <2 had respiratory and/or cardiac motion artifacts reported as the primary reason for reduced quality.

Comparison of 3D and 2D quantitative scar volumes in 20 randomly selected cases demonstrated a high level of agreement, with corresponding mean scar volumes of 11.2 ± 12.9% and 13.1 ± 14.5% of LV mass, respectively (R^2 = 0.88, slope 0.94).

Factors influencing image quality. Heart rate did not significantly impact image quality. Forty-four (80%) patients had heart rates of ≤80 beats/min during their studies. Studies performed during heart rates of ≤80 beats/min had mean segmental coronary artery and coronary vein quality scores of 2.7 ± 0.9 and 3.1 ± 0.9, respectively, whereas those performed at >80 beats/min had respective scores of 2.6 ± 0.9 and 3.0 ± 0.9 (p = 0.5 for both comparisons by 2-tailed *t* tests).

The mean respiratory navigator acceptance rate for coronary-enhanced and scar-enhanced imaging was 43 ± 9% and 43 ± 10%, respectively. The number of patients with respiratory navigator acceptance rates ≥40% was 28 (51%) for coronary imaging and 33 (60%) for 3D scar imaging. Studies performed with acceptance rates ≥40% had a mean quality score of 3.1 ± 0.7 for proximal–mid-arterial segments and 3.4 ± 0.8 for proximal–mid-vein segments. Respective values of 2.7 ± 0.8 and 3.1 ± 0.9 were found in studies with acceptance rates <40% (p < 0.0001 for coronary artery comparison and p = 0.03 for coronary vein comparison by 2-tailed *t* test). Quality scores for scar-enhanced images were 3.0 ± 0.8 and 2.5 ± 1.2 for acceptance rates ≥40% and ≤40%, respectively (p = 0.03 by 2-tailed *t* test).

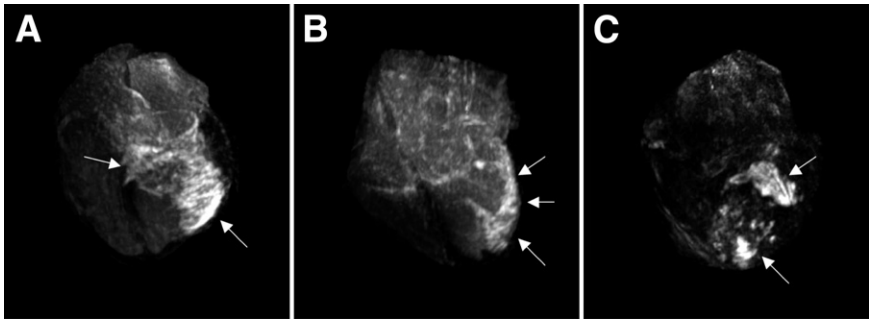

Figure 4. Examples of 3D High-Resolution Scar Maps

Patients with ischemic myocardial injury **(A and B)** and nonischemic (inflammatory) injury **(C)**. Scar indicated by white arrows. See accompanying Online Video 1. Abbreviation as in Figure 2.

Image segmentation and fusion. Of 44 studies demonstrating myocardial scar, 38 (86%) achieved successful image fusion. These were reliably obtained from the 36 patients (23 referred for CRT and 13 referred for CAR) achieving a 3D scar quality score ≥2. Six studies had suboptimal 3D scar segmentation owing to reduced image quality (quality score <2) and were not able to be fused. Examples of fused imaging in patients with ischemic, midwall, and epicardial-based scar patterns are shown in Figure 5. Both coronary artery and vein systems were clearly visualized relative to myocardial scar on volume-rendered images (Online Videos 2A, 2B, and 3).

Clinical relevance of 3D fused imaging. The presence of ≥1 vascular target with underlying transmural scar (>50% wall thickness) was seen in 17 of the 36 patients with fused imaging. This group consisted of 9 of 23 patients (39%) referred for CRT and 8 of 13 (62%) patients referred for CAR (Fig. 6).

Incremental clinical impact (clinical impact score ≥2) was recorded in 24 of the 36 patients (67%) undergoing successful image fusion. Examples of studies scored with impact scores ≥2 are shown in Figure 6. The mean impact score for therapeutic decision making was 2.8 ± 0.8 and 3.1 ± 0.7 in CRT and CAR patients, respectively. Procedures were canceled (clinical impact score of 4) owing to the results of imaging in 6 patients: 2 planned for CRT and 4 planned for CAR.

DISCUSSION

This study is the first to demonstrate the feasibility of matched, isotropic 3D imaging of coronary vasculature and myocardial scar using a single imaging modality. Fused volumetric display of these structures poses advantages for the spatial registration of vascular targets and related myocardial scar and was demonstrated to have a significant clinical impact on therapeutic decisions in patients referred for both CRT and CAR. This suggests a potential of this technique to meaningfully assist in the planning of vascular-based therapies reliant upon regional myocardial scar for clinical success.

Whole-heart coronary artery imaging using a continuous gadolinium infusion has been previously demonstrated at both 1.5-T (16–18) and 3-T (11,19–21) field strengths. Its ability to provide for evaluation of the coronary veins has also been reported at 1.5-T (22–24). The inversion-recovery technique used to provide myocardial signal suppression in this approach was adopted from the DE technique, initially described by Simonetti et al. (25). A lower TI is employed to accommodate for the shorter T1 relaxation seen during contrast

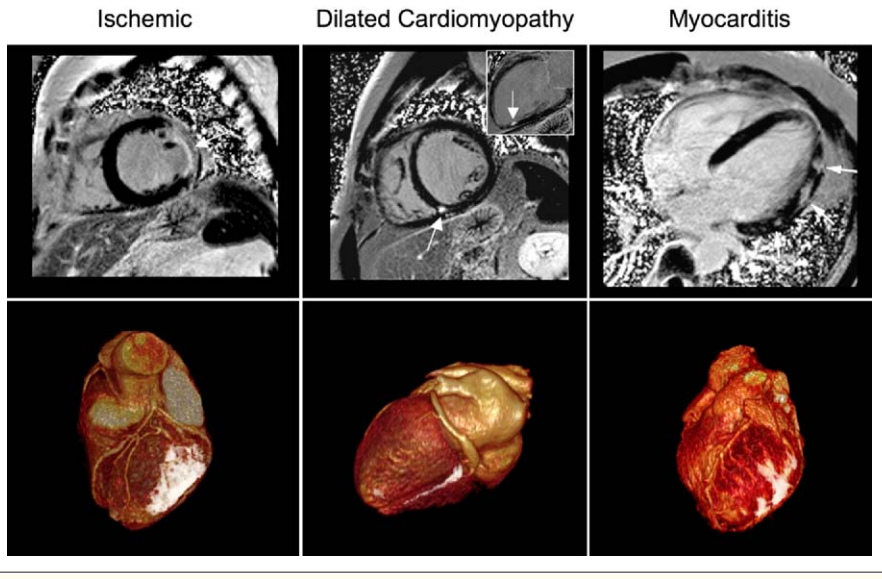

Figure 5. Demonstration of Varying Patterns of Myocardial Injury

Patterns of myocardial injury illustrated by conventional 2-dimensional late enhancement imaging **(top row)** and by fused, high-resolution 3-dimensional scar-coronary imaging **(bottom row)**. Ischemic: lateral wall myocardial infarction from ostial occlusion of ramus intermedius in patient referred for coronary artery bypass grafting. Dilated cardiomyopathy: midwall scar in patient with nonischemic dilated cardiomyopathy planned for cardiac resynchronization therapy. The **inset** shows small embolic infarction in apical segment of the inferior wall). Myocarditis: epicardial-based enhancement seen, consistent with prior myocarditis.

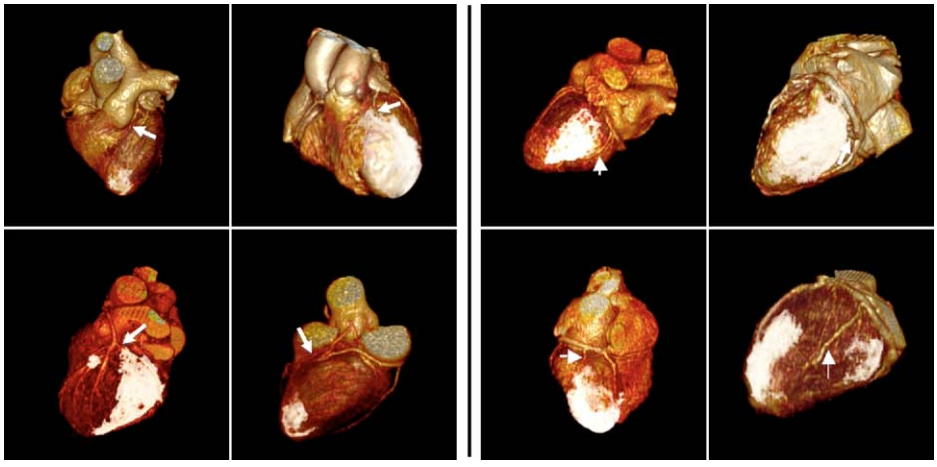

Figure 6. Examples of Scar-Coronary MRA Images Scored as Having Clinically Significant Impact

Example images from 4 patients planned for coronary revascularization **(left panel)** and 4 patients planned for cardiac resynchronization therapy **(right panel)** scored as having a clinically significant impact on planned therapy. Target vessels for the respective procedures are indicated by **white arrows**. See accompanying Online Videos 2A, 2B, and 3. Abbreviation as in Figure 3.

infusion (26). The current study demonstrates that a spatially matched 3D scar evaluation can be readily obtained following this coronary imaging technique using an isolated adjustment of the TI time. Semiautomated segmentation of these data can then be performed using widely available open source software (13) for rapid fusion to the 3D coronary MRA dataset.

Prior studies have demonstrated the improved signal characteristics of 3-T CMR in comparison with 1.5-T for the performance of 2D DE imaging (27). The clinical feasibility of high-resolution 3D scar imaging at 3-T has also been recently described (28). However, the current study demonstrates the clinical feasibility of isotropic myocardial scar imaging, an important advance for facilitation of 3D visualization. Although the approach of fusing multiple 2D scar images to a single 3D coronary dataset could also be considered, the current approach of using a matched 3D scar dataset offers high-resolution isotropic voxels with inherent registration, both spatially and temporally (within the cardiac cycle), affording rapid image fusion.

The incremental value of fusing scar to coronary imaging should be considered in the context of therapies likely to benefit from spatially relating these structures. The established and expanding role of CRT in patients with systolic heart failure is challenged by recognition of its limited or absent benefit in approximately one-third of patients (29,30). The presence of myocardial scar in either of the posterolateral or septal walls has been shown to negate the clinical benefit of CRT in these patients (6,7). Therefore, although the use of anatomic vascular imaging to plan placement of CRT leads has been recently suggested (3–5), the ability to simultaneously visualize this anatomy in the context of myocardial scar greatly enhances the identification of optimal targets.

Similarly, myocardial scar is intimately coupled to a lack of functional improvement following surgical and percutaneous revascularization (31–33). A fused 3D visual display of coronary anatomy and scar was shown to impact therapeutic decisions related to CAR in this study. In 2 such cases, LV remodeling surgery (Dor procedure [34]) was additionally performed following clear visualization of an isolated apical scar on fused imaging (Online Video 2A).

Study limitations. This study was not designed to evaluate the diagnostic accuracy of whole-heart coronary magnetic resonance angiography (MRA) for the detection of obstructive coronary disease. Such a study was recently performed by Yang et al. (21) using a similar MRA technique and showed promising results. However, it is not anticipated that MRA diagnostic accuracy will contribute to the clinical utility of the currently described technique because all patients planned for CAR will have already received invasive coronary imaging. The described technique's value is focused on the spatial registration of established vascular targets to regional scar.

Supplemental heart rate–reducing agents or sublingual nitrates were not used within this protocol; each agent has been previously used for optimiza-

tion of coronary artery imaging (35,36). However, a significant proportion (77%) of patients were receiving oral beta-blockers. Image quality might also be further improved through the use of 32-channel coil technology, which has recently been shown to be beneficial for coronary imaging at 3-T field strengths (37).

CONCLUSIONS

The performance of 3D isotropic myocardial scar imaging with fusion to spatially matched coronary imaging is clinically feasible. This novel imaging approach has potential for providing clinical impact on the planning of vascular-based cardiac interventions in which myocardial scar is considered relevant to therapeutic success.

Reprint requests and correspondence: Dr. James A. White, Cardiovascular MRI Clinical Research (CMCR) Program, 3T-7T MRI Unit, Robarts Research Institute, P.O. Box 5015, 100 Perth Drive, London, Ontario, N6A 5K8 Canada. *E-mail: jwhite@imaging.robarts.ca.*

REFERENCES

1. Gulbins H, Reichenspurner H, Becker C, et al. Preoperative 3D-reconstructions of ultrafast-CT images for the planning of minimally invasive direct coronary artery bypass operation (MIDCAB). Heart Surg Forum 1998;1:111–5.
2. Gasparovic H, Rybicki FJ, Millstine J, et al. Three dimensional computed tomographic imaging in planning the surgical approach for redo cardiac surgery after coronary revascularization. Eur J Cardiothorac Surg 2005;28:244–9.
3. Van de Veire NR, Schuijf JD, De Sutter J, et al. Non-invasive visualization of the cardiac venous system in coronary artery disease patients using 64-slice computed tomography. J Am Coll Cardiol 2006;48:1832–8.
4. Singh JP, Houser S, Heist KE, Ruskin JN. The coronary venous anatomy. A segmental approach to aid cardiac resynchronization therapy. J Am Coll Cardiol 2005;46:68–74.
5. Rioual K, Unanua E, Laguitton S, et al. MSCT labeling for pre-operative planning in cardiac resynchronization therapy. Comput Med Imaging Graph 2005;29:431–9.
6. Bleeker GB, Kaandorp TA, Lamb HJ, et al. Effect of posterolateral scar tissue on clinical and echocardiographic improvement after cardiac resynchronization therapy. Circulation 2006;113:969–76.
7. White JA, Yee R, Yuan X, et al. Delayed enhancement magnetic resonance imaging predicts response to cardiac resynchronization therapy in patients with intraventricular dyssynchrony. J Am Coll Cardiol 2006;48:1953–60.
8. Ypenburg C, Schalij MJ, Bleeker GB, et al. Impact of viability and scar tissue on response to cardiac resynchronization therapy in ischemic heart failure patients. Eur Heart J 2007;28:33–41.
9. Kim RJ, Wu E, Rafael A, et al. The use of contrast-enhanced magnetic resonance imaging to identify reversible myocardial dysfunction. N Engl J Med 2000;343:1445–53.
10. Beek AM, Kuhl HP, Bondarenko O, et al. Delayed contrast-enhanced magnetic resonance imaging for the prediction of regional functional improvement after acute myocardial infarction. J Am Coll Cardiol 2003;42:895–901.
11. Bi X, Carr JC, Li D. Whole-heart coronary magnetic resonance angiography at 3 Tesla in 5 minutes with slow infusion of Gd-BOPTA, a high-relaxivity clinical contrast agent. Magn Reson Med 2007;58:1–7.
12. Kim RJ, Shah DJ, Judd RM. How we perform delayed enhancement imaging. J Cardiovasc Magn Reson 2003;5:505–14.
13. OsiriX Imaging Software. Available at: http://www.osirix-viewer.com/. Accessed May 29, 2009.
14. Scalon PJ, Faxon DP, Audet AM, et al. ACC/AHA guidelines for coronary angiography: executive summary and recommendations—a report of the American College of Cardiology/American Heart Association Task Force on Practice Guidelines (Committee on Coronary Angiography) developed in collaboration with the Society for Cardiac Angiography and Interventions. Circulation 1999;99:2345–57.
15. Alderman EL, Stadius M. The angiographic definitions of the Bypass Angioplasty Revascularization Investigation. Coron Artery Dis 1992;3:1189–207.
16. Goldfarb JW, Edelman RR. Coronary arteries: breath-hold, gadolinium enhanced, three-dimensional MR angiography. Radiology 1998;206:830–4.
17. Kessler W, Laub G, Achenbach S, Ropers D, Moshage W, Daniel WG. Coronary arteries: MR angiography with fast contrast-enhanced three-dimensional breath-hold imaging—initial experience. Radiology 1999;210:566–72.
18. Li D, Carr JC, Shea SM, et al. Coronary arteries: magnetization-prepared contrast-enhanced three-dimensional volume-targeted breath-hold MR angiography. Radiology 2001;219:270–7.
19. Bi X, Li D. Coronary arteries at 3.0 T: contrast-enhanced magnetization-prepared three-dimensional breath-hold MR angiography. J Magn Reson Imaging 2005;21:133–9.
20. Liu X, Bi X, Huang J, Jerecic R, Carr J, Li D. Contrast-enhanced whole-heart coronary magnetic resonance angiography at 3.0 T: comparison with steady-state free precession technique at 1.5 T. Invest Radiol 2008;43:663–8.
21. Yang Q, Li K, Liu X, et al. Contrast-enhanced whole-heart coronary magnetic resonance at 3.0-T: a comparative study with X-ray angiography in a single center. J Am Coll Cardiol 2009;54:69–76.
22. Rasche V, Binner L, Cavagna F, et al. Whole-heart coronary vein imaging: a comparison between non-contrast-agent- and contrast-agent- enhanced visualization of the coronary venous system. Magn Reson Med 2007;57:1019–26.
23. Chiribiri A, Kelle S, Gotze S, et al. Visualization of the cardiac venous system using cardiac magnetic resonance. Am J Cardiol 2008;101:407–12.
24. Younger JF, Plein S, Crean A, Ball SG, Greenwood JP. Visualization of coronary venous anatomy by cardiovascular magnetic resonance. J Cardiovasc Magn Reson 2009;11:26–34.
25. Simonetti O, Kim RJ, Fieno DS, et al. An improved MR imaging technique for the visualization of myocardial infarction. Radiology 2001;8:215–23.

26. Zheng J, Li D, Bae KT, Woodard P, Haacke EE. Three-dimensional gadolinium enhanced coronary magnetic resonance angiography: initial experience. J Cardiovasc Magn Reson 1999; 1:22–41.
27. Klumpp B, Fenchel M, Hoevelborn T, et al. Assessment of myocardial viability using delayed enhancement magnetic resonance imaging at 3.0 Tesla. Invest Radiol 2006;41:661–7.
28. Amano Y, Matsumura Y, Kumita S. Free-breathing high-spatial resolution delayed contrast-enhanced three-dimensional viability MR imaging of the myocardium at 3.0T: a feasibility study. J Magn Reson Imaging 2008; 28:1361–7.
29. Cleland JG, Daubert JC, Erdmann E, et al. The effect of cardiac resynchronization on morbidity and mortality in heart failure. N Engl J Med 2005;352: 1539–49.
30. Leclerq C, Kass DA. Retiming the failing heart: principles and current status of cardiac resynchronization. J Am Coll Cardiol 2002;39:194–201.
31. Ragosta M, Beller GA, Watson DD, Kaul S, Gimple LW. Quantitative planar rest-redistribution 201Tl imaging in detection of myocardial viability and prediction of improvement in left ventricular function after coronary bypass surgery in patients with severely depressed left ventricular function. Circulation 1993;87:1630–41.
32. Arnese M, Cornel JH, Salustri A, et al. Prediction of improvement of regional left ventricular function after surgical revascularization: a comparison of low-dose dobutamine echocardiography with 201Tl single-photon emission computed tomography. Circulation 1995;91:2748–52.
33. Pagley PR, Beller GA, Watson DD, Gimple LW, Ragosta M. Improved outcome after coronary bypass surgery in patients with ischemic cardiomyopathy and residual myocardial viability. Circulation 1997;96:793–800.
34. Dor V, DiDonato M, Sabatier M, Montiglio F, Civaia F, RESTORE Group. Left ventricular reconstruction by endoventricular circular patch plasty repair: a 17-year experience. Semin Thorac Cardiovasc Surg 2001; 13:435–47.
35. Jahnke C, Paetsch I, Achenbach S, et al. Coronary MR imaging: breath-hold capability and patterns, coronary artery rest periods and beta-blocker use. Radiology 2006;239:71–8.
36. Leschka S, Wildermuth S, Boehm T, et al. Noninvasive coronary angiography with 64-section CT: effect of average heart rate and heart rate variability on image quality. Radiology 2006;241:378–85.
37. Niendorf T, Hardy CJ, Giaquinto RO, et al. Toward single breath-hold whole-heart coverage coronary MRA using highly accelerated parallel imaging with a 32-channel MR system. Magn Reson Med 2006;56:167–76.

Key Words: cardiac magnetic resonance ■ coronary imaging ■ delayed enhancement ■ image fusion.

APPENDIX

For supplementary videos and their legends, please see the online version of this article.